⁘ *Title (50 w)*

Plasticity of the dopaminergic phenotype and of locomotion in larval zebrafish induced by changes in brain excitability during the embryonic period.

Embryonic excitability modulates differentiation

Sandrine Bataille*[1], Hadrien Jalaber*[1], Ingrid Colin*[1], Damien Remy[1], Pierre Affaticati[2], Cynthia Froc[1], Philippe Vernier[1] and Michaël Demarque**[1].

1. Paris Saclay Institute of Neuroscience, (UMR9197) CNRS and Université Paris-Saclay; Avenue de la Terrasse, 91190 Gif-sur-Yvette, France

2. TEFOR Paris-Saclay, CNRS UMS2010 / INRAE UMS1451, Université Paris-Saclay, Avenue de la Terrasse, 91190 Gif-sur-Yvette, France

*authors contributed equally

**Corresponding author

⁘ *Corresponding author email address: michael.demarque@cnrs.fr*

⁘ *Number of pages: 39*

⁘ *Number of figures, tables, multimedia, and 3D models (separately): 6/0/0/0*

⁘ *Number of words for abstract, introduction, and discussion: 233/646/1261*

⁘ *Conflict of interest statement:* The authors declare no competing financial interests.

⁘ *Acknowledgments:* This work was funded by the French National Research Agency (ANR project “PallEnody”) and the Fondation pour la Médicale Recherche, FRM (“team FRM”). The authors thank Kei Yamamoto for scientific inputs, TEFOR Paris Saclay (TPS) for technical support.

ABSTRACT (233/250 w):

During the embryonic period, neuronal communication starts before the establishment of the synapses with forms of neuronal excitability, called here Embryonic Neuronal Excitability (ENE). ENE has been shown to modulate the correct unfolding of development transcriptional programs but the global consequences for the developing organisms are not all understood. Here we monitored calcium transients in zebrafish embryos as a proxy for ENE to assess the efficacy of transient pharmacological treatments able to either increase or decrease ENE. Increasing or decreasing ENE for 24 hour at 2 days post fertilization (dpf) promoted respectively an increase or decrease in the post-mitotic differentiation of the dopamine (DA) neurons in the telencephalon and in the olfactory bulb of zebrafish larvæ at 6 dpf. This plasticity of dopaminergic specification occurs within a stable population of vMAT2 immuno-reactive cells, hence identifying an unanticipated biological marker for this pool of reserve cells, that can be recruited through ENE.

Modulating ENE also affected locomotion several days after the end of the treatments. In particular, the increase of ENE from 2 to 3 dpf promoted an hyperlocomotion in 6 dpf zebrafish larvæ, reminiscent of endophenotypes reported for Attention Deficit with Hyperactivity Disorders and schizophrenia in zebrafish. These results provide a convenient framework to identify environmental factors that could disturb ENE as well as to study the molecular mechanisms linking ENE to the neurotransmitters specification, with clinical relevance for the pathogenesis of neurodevelopmental disorders.

Significance Statement (109/ 120 w):

- Spontaneous calcium spikes, used as a proxy for Embryonic Neuronal Excitability (ENE), are detected in the forebrain of embryonic zebrafish.
- Transients pharmacological treatments applied by balneation could be used to increase or decrease ENE.
- The post-mitotic differentiation of the dopaminergic phenotype is modulated by ENE in the zebrafish forebrain.
- The plasticity of the dopaminergic specification occurs within a reserve pool of vMAT2 immuno-reactive cells.
- Transient increase of ENE at the end of the embryonic period induces a hyperlocomotion, a phenotype associated with ADHD and schizophrenia in this model.
- Our results open clinically relevant perspectives to study the pathogenesis of neurodevelopmental disorders in zebrafish.

Introduction (646/650 w)

During brain development, specific molecular components of the synaptic neuronal communication such as ion channels, neurotransmitters and neurotransmitter receptors are expressed and functional before synapse formation (Spitzer et al., 2002). They contribute to immature forms of cellular excitability and intercellular communications we propose to refer to as Embryonic Neuronal Excitability (ENE). There is for instance a paracrine communication mediated by activation of receptors by endogenous neurotransmitters, GABA and glutamate, in the neonatal rat hippocampus, or glycine in the mouse spinal cord (Demarque et al., 2002; Owens & Kriegstein, 2002; Scain et al., 2010). Acute changes of calcium concentration have also been described, including filopodial or growth cone transients, and calcium spikes

70 in differentiating neurons (Gomez & Spitzer, 1999; Gomez et al., 2001; Borodinsky et
71 al., 2004). Calcium spikes are sporadic, long lasting global increase of intracellular
72 concentration of Ca^{2+} that occurs during restricted developmental windows called
73 "critical periods". They have been identified in the developing brain of several
74 vertebrate species (Owens & Kriegstein, 1998; Borodinsky et al., 2004; Crepel et al.,
75 2007; Blankenship & Feller, 2010; Demarque & Spitzer, 2010; Warp et al., 2012;
76 Plazas et al., 2013). Quantification of calcium spikes by calcium imaging can be used
77 as proxy for ENE. Changes in the incidence and frequency of calcium spikes modulate
78 the specification of the neurotransmitter phenotype in neurons, as it is the case for
79 dopamine (DA), in several cell populations of the xenopus and mouse brain, with
80 consequences on several behaviors (Dulcis & Spitzer, 2008; Dulcis et al., 2013, 2017).
81 DA is an evolutionary conserved monoamine involved in the neuromodulation of
82 numerous brain functions in vertebrates, including motivational processes, executive
83 functions and motor control (Klein et al., 2019). Accordingly, alterations of the
84 differentiation and function of the neurons synthetizing DA contribute to the
85 pathogenesis of several brain disease with a neurodevelopmental origin, such as
86 Attention Deficit Hyperactivity Disorder (ADHD) and schizophrenia (SZ) (Lange et al.,
87 2012; Murray et al., 2017).
88 Further addressing the complex molecular and cellular mechanisms linking
89 developmental excitability, dopaminergic differentiation and behavioral outputs
90 requires an *in vivo* approach in a model accessible, genetically amenable and with
91 possible parallels with the human situations. The developing zebrafish *Brachydanio*
92 *rerio* fits with these needs. The development of the embryos is external, which allows
93 inducing perturbations of ENE at stages that would be *in utero* in mammalian models.
94 The embryos are relatively small and transparent, simplifying high-resolution imaging

of the brain in live or fixed preparations. Despite difference in the brain organization, notably a pallium very different form the 6-layered cortex of mammals, the main neuronal systems of vertebrates are present in zebrafish and respond to psychoactive drugs (Gawel et al., 2019). In addition, the monoaminergic system has been extensively studied in zebrafish (Schweitzer & Driever, 2009; Schweitzer et al., 2012). In vertebrates, DA modulates executive functions, such as working memory and decision making, through innervation of specific regions of the telencephalon. In the zebrafish brain, most DA neurons innervating the telencephalon have their cell bodies located within the telencephalon itself (TelDA cells) (Tay et al., 2011; Yamamoto et al., 2011). To the best of our knowledge, there is no evidence for a plasticity of the neurotransmitter phenotype in these cells.

To perturb ENE in conditions close to physiological exposure and ecotoxicology, we used pharmacological treatments by balneation from 48 to 72 hours post fertilization (hpf). We then analyzed the consequences of these transient pharmacological treatments a few days later, between 6 and 7 dpf. We report quantifiable changes in the specification of the dopaminergic phenotype in TelDA neurons. We also report changes for high-speed swimming episodes. These results suggest a role of ENE on the specification of the dopaminergic phenotype and motor control in the zebrafish. They also open important perspectives for this model to decipher the chain of events leading from environmental factors to the pathogenesis of disorders such as schizophrenia and ADHD.

117 **Materials and Methods**

118 **Fish strains**

119 All experiments were carried out in accordance with animal care guidelines
120 provided by the French ethical committee and under the supervision of authorized
121 investigators.

122 Zebrafish were raised according to standards procedures. Briefly, for breeding,
123 males and females zebrafish were placed overnight, in different compartments of a
124 tank with a grid at the bottom that allows the eggs to fall through. The next morning the
125 separation was removed and after few minutes, the eggs were collected, rinsed and
126 placed in a petri dish containing embryo medium (EM). Embryos were kept at
127 28 degrees, then staged as hours post fertilization according to specific criteria. The
128 number of animal used for each experiments is indicated in the corresponding figure
129 legends.

130 **Pharmacological treatments**

131 Pharmacological compound, veratridine (10 μM), TTX (2 μM), ω conotoxin
132 (0.08 μM), nifedipine (0.4 μM) and flunarizine (2 μM) were purchased form R&D
133 System (UK) and prepared in water except veratridine which required dimethyl
134 sulfoxide (DMSO) for dissolution and flunarizine that requires ethanol for dissolution.
135 Sham control were performed using the same concentration of DMSO in EM without
136 the drug to rule out an effect of the detergent itself. Specific period and duration of
137 applications are indicated in the corresponding figure legends. All pharmacological
138 treatments were performed by balneation followed by three washes in EM. Embryos
139 were randomly distributed in wells (30 embryos per well) of a 6-well plate containing
140 5 mL of solution (EM+DMSO or EM+drug). Embryos exposed to drugs or the sham
141 control solution were observed for morphological abnormalities every day until 5 dpf.

142 Malformations (*e.g*. spinal curvature, cardiac edema) were considered as experimental
143 end-points and when detected the corresponding animals were excluded from the
144 study.

145 **Calcium imaging**

146 At 24 hpf embryos of the (Hsp70:GAl4 x UAS:GCaMP6f;cry:mCherry) line were
147 exposed to a 38°C temperature for 1.5 hour. Upon heat shock activation, GCamp6f is
148 expressed in all the cells of the animals.

149 At 2-3 dpf the embryos were then individually embedded in low melting agarose,
150 ventral side up for imaging.

151 30 min time lapse series were acquired at 1 Hz, at a single focal plane, on an
152 Olympus BX60 microscope (Olympus corporation, Tokyo, Japan) equipped with a
153 40x 0.6N water immersion objective. A non-laser spinning disk system (DSD2, ANDOR
154 Technology, Oxford, UK) was used for illumination and image acquisition. Images were
155 open in Fiji and analyzed using Multi Measure (W. Rasband, B. Dougherty), Measure
156 Stack (Optinav, Redmond, WA), and custom Image J plugins. Regions of interest
157 (ROIs) were drawn manually over individual cell bodies. Movements of the preparation
158 in the X/Y axis were corrected using the plugin Measure Stack. Average gray level
159 from pixels in ROIs was measured over time. Spikes were defined as increase of
160 fluorescence higher than 2 times the standard deviation of the baseline. The duration
161 of spikes was calculated as the width at half-maximum. Incidence was scored as the
162 number of cells generating transients divided by the estimated total number of cells in
163 the imaged field and was expressed as a percentage. Frequency was calculated as
164 the total number of transients in a given cell divided by the total acquisition time and
165 was expressed as spikes per hour.

166 **Immunohistochemistry**

167 *Tissue preparations*

168 6-7 dpf zebrafish larvæ were deeply anesthetized using 0.2% Ethyl3-
169 amniobenzoate methanesulfonate (MS222; Sigma-Aldrich) diluted in EM, then they
170 were fixed in ice-cold 4% paraformaldehyde (PFA; Electron Microscopy Sciences) in
171 1X phosphate-buffered saline (PBS; Fisher Scientific) containing 0.1% Tween 20 %
172 (PBST) overnight at 4 °C. Samples were dehydrated and stored in MeOH at -20°C.

173 *Immunofluorescence*

174 Immunofluorescence was performed in 2 mL microtubes. Unless specified
175 otherwise in the protocol, incubations were performed at room temperature (RT), and
176 thorough PBST washes were performed between each steps. The samples were first
177 incubated in 3% Hydrogen Peroxide Solution (H_2O_2) in Ethanol 100% (EtOH) for
178 30 minutes, to deactivate endogenous peroxidases. They were then successively
179 incubated in EtOH:Xylen 1:1 without agitation for 1 hour and, at -20 °C, in
180 EtOH:Aceton 1:2 without agitation for 20 minutes. The washes were performed
181 between these steps were performed in EtOH. After the final wash, samples were
182 rehydrated in PBST.

183 In order to unmask the antigens, samples were incubated in PBST:Tris 150 mM
184 pH9 for 10 minutes, then in Tris 150 mM pH9 at RT for 10 minutes and at 70 °C for
185 30 minutes. After PBST washes, the samples were incubated in a blocking buffer
186 (10% normal goat serum (NGS), 1% triton X-100, 1% tween-20, 1% DMSO,
187 1% Bovin Serum Albumin (BSA) in PBS 1X) for 3 hours.

188 Two protocols were used for primary antibody staining. For the TH antibody, the
189 samples were incubated with the first primary antibody (mouse anti-TH, 1:250) in a
190 staining solution (1% NGS, 1% triton X-100, 1% DMSO, 1% BSA, 0,05% azide sodium

191 in PBST) at 4°C for 7-10 days, under gentle agitation. The samples were then
192 incubated in a blocking buffer DAB (4% NGS, 0,3% triton X-100, 0,5% DMSO in PBST)
193 for 1 hour at RT and incubated with a first secondary antibody (anti-mouse biotinylated,
194 1:200) in a secondary staining buffer (4%NGS, 0,1% triton X-100 in PBST) for 2,5 days
195 at 4°C under gentle agitation.

196 For the revelation, we used the Vectastain ABC kit (Vector ®).Briefly, a AB mix
197 was prepare by adding 10 µl of solution A and 10 µl of solution B in 1mL PBST/1%
198 Triton-X100. One hour after the preparation, the samples were incubated in the AB mix
199 for 1 hour. Samples were then incubated in Tyramid-TAMRA (1:200 in PBST) for
200 20 minutes, then 0,012% H_2O_2 was added directly in the solution and the samples
201 were incubated for an additional 50 minutes.

202 Before a second primary antibody incubation, the samples underwent a step of fixation
203 in PFA 4% for 2 hours at RT and washed overnight in PBST.

204 For the other primary antibodies (rabbit anti-caspase3, 1:500 or chicken anti-GFP,
205 1:500), the samples were incubated in the blocking buffer (1 hour when following a TH
206 staining, 3 hours otherwise), then they were incubated with the primary antibody in a
207 staining solution at 4 °C for 3-4 days, under gentle agitation. After washes, the samples
208 were incubated with the second secondary antibody (goat anti-chicken Alexa Fluor
209 488, 1:500) and DAPI 1X in PBST at 4 °C for 2,5 days under gentle agitation. Samples
210 were then washed three times in PBST and left overnight in PBST. For observation,
211 the brain were dissected and mounted between slides and coverslides in Vectashield
212 solution (Vector®).

213 *Image acquisition*

214 A Leica TCS SP8 laser scanning confocal microscope with a Leica HCTL Apo
215 × 40/1.1 w objective was used to image the specimens.

216 Fluorescence signal was detected through laser excitation of fluorophores at 405, 488,
217 552, or 638 nm and detection was performed by two internal photomultipliers. Steps in
218 the Z-axis were fixed at 1 µm. Acquired images were adjusted for brightness and
219 contrast using ImageJ/FIJI software.

220 *Quantification of immuno-reactive cells*

221 The TH- and GFP-IR cells were counted manually from z-stacks of confocal
222 images using the ImageJ cell counter plugin.

223 **Spontaneous locomotion assays**

224 Individual larvæ were placed in a well of a 24 well plate with 2 mL EM 2 hours
225 before recordings for habituation. The plate is then placed in a Zebrabox (Viewpoint,
226 Lyon, France) for 10 minutes recording sessions. Locomotor activity was recorded
227 using ZebraLab software (Videotrack; ViewPoint Life Sciences, France). After a first
228 session without threshold for 24 untreated larvæ the average speed (av_sp) of the
229 batch was extracted from the data. For subsequent sessions, two threshold were
230 applied. Swim bouts with a speed below half the average speed (av_sp/2) were
231 considered as inactivity, episodes with a speed over twice the average speed
232 (av_sp*2) were considered as fast episode or burst and episodes with a speed
233 between the two threshold were considered as cruises episodes or normal swim.

234 For each sessions, each animal and each category of episodes (inactivity, cruises
235 epiosdes and bursts episodes), 4 parameters are extracted from the recordings: the

236 number of episodes, the total distance covered, the duration of activity, and the
237 average speed.

238 Experimental design

239 Statistical analyses

240 Results are shown as means ± SEM. Means comparisons were performed using
241 the appropriate non parametric statistical tests (ANVOA, Mann Whitney U test or
242 Kruskal-Wallis test depending on the experimental conditions). $P < 0.05$ was
243 considered statistically significant and noted as follow: $P < 0.05$ (*), $P < 0.01$ (**),
244 $P < 0.001$ (***).

245 For percentages, we used the 95% confidence interval defined as
246 =1.96*squareroot((x*(1-x)/n)), n being the number of independent samples and x being
247 the % of change observed.

248 All statistical tests were performed using the online software Brightstat and R.

249 Results

250 Presence of calcium spikes in the brain of zebrafish embryo.

251 To study Embryonic Neuronal Excitability (ENE) in the embryonic zebrafish brain,
252 we recorded calcium spikes as a proxy. To follow the dynamics of intracellular calcium
253 concentration we used the (Hsp70:GAl4 x UAS:GCaMP6f;cry:mCherry) transgenic
254 line, in which the genetically encoded calcium reporter GCamp is expressed upon heat
255 shock activation (see Materials and Methods). To monitor changes in fluorescence
256 over time, we performed time-lapse imaging of the anterior most part of the brain of 2-
257 3 dpf zebrafish embryos for 30 minutes sessions.

258 Spontaneous changes in fluorescence were detected in forebrain cells, likely
259 including presumptive dopaminergic cells in the telencephalon and the OB (Figure 1A).
260 We analyzed the evolution of the fluorescence from selected regions of interest
261 corresponding to individual cell bodies (Figure 1B and Materials and methods). The
262 average frequency of the recorded Ca^{2+} spikes was 6.6+/-5.4 spikes.h-1; the average
263 incidence of these events was 45.2+/-9.7%; these events had a mean duration of
264 3.3/+- 1.6 s (n= 28 spikes from 5 independent preparations Figure 1C, blue boxplots).
265 These parameters are in the range of what has been reported in the zebrafish spinal
266 cord, confirming that the duration of Ca^{2+} spikes is shorter in zebrafish than in xenopus
267 (Dulcis & Spitzer, 2008; Warp et al., 2012; Plazas et al., 2013).

268 **Global pharmacological modifications of calcium spikes dynamics**

269 In order to assess the effects of global manipulations of ENE, we applied
270 pharmacological compounds directly in the embryo medium. The treatments were
271 performed during the last day of embryonic development (48-72 hpf) to reduce the
272 effects on early developmental steps such as neurulation and proliferation. These
273 drugs were already used in *Xenopus* for similar purposes (Borodinsky et al., 2004). To
274 increase calcium spiking we used veratridine (10 µM), which blocks the inactivation of
275 voltage-dependent sodium channels. To decrease calcium spiking, we used a cocktail
276 containing TTX (2 µM), ω-Conotoxin (0.08 µM), Nifedipine (0.4 µM) and Flunarizine
277 (2 µM) targeting respectively voltage-dependent sodium channels; N, L and T subtypes
278 of voltage dependent calcium channels (we refer to this cocktail as TCNF based on
279 the initials of its 4 components).

280 We performed time-lapse recordings of the (Hsp70:GAl4 x
281 UAS:GCaMP6f;cry:mCherry) transgenic line two to ten hours after the beginning of the
282 treatments.

283 Following either veratridine treatment (n=26 spikes from 4 independent
284 preparations) or TCNF treatment (n=15 from 4 independent preparations), individual
285 events had a similar duration as in control (Kruskal-Wallis test, p=0.538; Figure 1C).
286 Following veratridine treatments, the average frequency of calcium spikes was
287 increased (+39.3+/-16%, n=36 cells from 4 independent preparations, p=0.206
288 bonferroni post-hoc test) as well as the average incidence of calcium transients
289 (29.9+/-45% n=4 independent preparations, p<0.05 conover posthoc comparisons;
290 Figure 1C, green boxplots).

291 Following TCNF treatments, the average frequency of calcium spikes was
292 decreased (-29+/-22%, n=17 cells from 4 independent preparations, p=0.812
293 bonferroni post-hoc test) as well as the average incidence (-44+-/48% n=4
294 independent preparations, p<0.01 Kruskal-Wallis paired comparisons)(Figure 1C, red
295 boxplots).

296 These results demonstrate that balneation treatments are able to change the
297 incidence and frequency of spontaneous calcium spikes in the embryonic zebrafish
298 forebrain. Based on these results, we refer to veratridine treatment as “increase of
299 ENE”, and to TCNF treatment as “decrease of ENE”, in the following sections of the
300 manuscript.

301 **Dopaminergic cells in the telencephalon and the olfactory bulb (OB) in the**
302 **zebrafish brain at larval stages.**

303 To identify dopaminergic neurons in the telencephalon and the OB, we used two
304 markers of the catecholaminergic phenotype, immune-labeled tyrosine hydroxylase 1
305 (TH1), the rate limiting enzyme for dopamine synthesis and the vesicular monoamines
306 transporter (vMAT2) combined to anatomical landmarks such as the position of brain

307 ventricles or large fibers bundles. Indeed, in zebrafish, like in mammals, noradrenaline-
308 containing neuronal soma are not detected in the forebrain anterior to the midbrain-
309 hindbrain boundary, rather, they are restricted to neuronal subpopulations located in
310 the nucleus locus coeruleus, the medulla oblongata and the area postrema (Ma,
311 1994a; b, 1997, 2003). Thus, all the catecholaminergic neurons located in front of the
312 midbrain-hindbrain boundary are likely to be dopamine neurons.

313 To localize these markers we performed double wholemount
314 immunohistochemistry on 6-7 dpf larvæ of the Tg(Et.vMAT2:eGFP) transgenic line.
315 We used an anti-GFP antibody to amplify the endogenous GFP signal to visualize cells
316 expressing vMAT2 (referred to as vMAT2+ cells in the remaining of the manuscript)
317 and an anti-TH antibody to identify TH1 cells (referred to as TH1+ cells in the remaining
318 of the manuscript). This anti-TH antibody is specific to TH1 and does not have affinity
319 for TH2 (Yamamoto et al., 2011).

320 In control conditions, in the telencephalon, we detected 15.1+/-3.1 TH1+ cells
321 (n= 39 samples from 6 independent experiments; Figure 2A, left column, Figure 2B,
322 blue boxplot). The cell bodies of these neurons were distributed bilaterally along the
323 midline, and relatively close to it. The major pattern of fibers distribution we could detect
324 was that of fibers projecting first ventrally and then laterally joining the wide
325 dopaminergic lateral longitudinal tracts.

326 An average of 63.4+/-6.7 vMAT2+ cells was also detected in this region (n= 39
327 samples from 6 independent experiments; Figure 2A, blue boxed column, Figure 2 C
328 blue boxplot). The overall disposition of the cell bodies and projections was the same
329 as for TH+ cells.

330 In control conditions, in the OB, 46.4+/-8.1 vMAT2+ cells and 30+/-2.6 TH1+ cells
331 were detected (n= 39 samples from 6 independent experiments; Figure 2A, blue boxed
332 column and Figure 2D and 2E, blue boxplot). The cell bodies of these OB TH1+
333 neurons were distributed at the anterior end of the forebrain and they were initially
334 projecting in an anterior direction before rapidly branching in multiple directions.

335 In both regions, all TH1+ cells were also vMAT2+ while some vMAT2+ cells were
336 TH1-. In the telencephalon, vMAT2+/TH1- cell bodies were mostly located at the
337 anterior end of the cluster of vMAT2/TH1+ cells. Such $vMAT2^{+}/TH^{-}$ cells are also
338 detected in the telencephalon of adult zebrafish (Yamamoto et al., 2011). Thus, in the
339 developing zebrafish telencephalon, the population of $vMAT2^{+}$ cells slightly exceeds
340 that of TH1-expressing cells.

341 **Effects of pharmacological treatments on the expression of dopaminergic**
342 **markers in the telencephalon and the OB.**

343 To assess the effects of ENE on the expression of telencephalic dopaminergic
344 markers at larval stages, we applied pharmacological treatments by balneation from
345 48 to 72 hpf as described above and performed whole-mount immunohistochemistry
346 on larvæ fixed at 6-7 dpf.

347 Increasing the excitability in the zebrafish brain also increased the number of TH1+
348 cells both in the telencephalon and in the OB (+28.6+/-15%, $p<0.05$ and +45.9+/-17%
349 $p<0.001$ respectively, n=35 samples from 6 independent experiments, conover
350 posthoc comparisons, Figure 2A, green boxed column; Figure 2B and 2D, green
351 boxplots). Meanwhile, the number of vMAT2 cells did not change significantly in either
352 regions ($p=0.08$ for the telencephalon, $p=0.659$ for the OB, Kruskal wallis test; n=16
353 samples from 6 independent experiments; Figure 2A, green boxed column, Figure
354 2C,E, green boxplots).

355 Following decreased excitability, the number of TH1+ cells diminished in the
356 telencephalon but not in the OB (-14.5+/-9.6% and -0.7+/-7.3% respectively, n=49
357 samples from 6 independent experiments; $p<0.001$ and $p>0.05$ respectively, conover
358 posthoc comparisons, Figure 2A, red boxed column, Figure 2B and 2D, red boxplot).
359 Meanwhile, the number of vMAT2 cells did not change significantly in either regions
360 (Kruskal wallis test: $p=0.08$ for the OB, $p=0.659$ for the OB; n=24 from 6 independent
361 experiments; Figure 2A, red boxed column and Figure 2C and 2E, red boxplots). In
362 both experimental situations, that is, after increasing or decreasing ENE, all the TH1+
363 cells also exhibited vMAT2 labelling. Hence, according to our identification criteria
364 (anatomical position combined to the expression of TH and vMAT2), an increase of
365 embryonic electrical activity increases the number of TelDA cells, while a decrease of
366 embryonic electrical activity decreases the number of TelDA cells.

367 On the other hand, the number of vMAT2+ cells was relatively stable in comparison
368 to TH1+ cells following the perturbation of activity (only decreasing in the telencephalon
369 following a decrease of activity). The stability of the number of vMAT2+ cells and the
370 lower proportion of $vMAT2^{+}/TH^{-}$ cells following increase of ENE suggest that the cells
371 that express a complete dopaminergic phenotype in this condition are recruited among
372 a population of $vMAT2^{+}/TH^{-}$ cells. Hence $vMAT2^{+}/TH^{-}$ cells would behave as a reserve
373 pool for dopaminergic cells (Dulcis & Spitzer, 2012). A similar conclusion could also
374 apply to the OB, despite the fact that the number of TH1+ cells is not statistically
375 diminished following decreased activity in this region. This unexpected result could
376 account for a number of TH1+ cells already set at a minimum in basal conditions in the
377 OB.

378 **Modifications of ENE do not have an effect on cell death in the forebrain**

379 To check whether increase or decrease of ENE could change cell survival, we

380 counted the number of cells IR for the apoptosis marker caspase-3 at 6-7 dpf. The
381 number of caspase-3+ cells was stable following the increase or the decrease of ENE,
382 strengthening the hypothesis that the changes observed in the number of TH1+ cells
383 is indeed linked to changes in specification rather than changes in cell death (Figure 3).

384 **Maturation of spontaneous swimming in zebrafish larvæ**

385 In order to analyze the consequence of changes in ENE on motor behaviors in
386 zebrafish larvæ, we recorded swimming episodes, as described in Materials and
387 Methods. During locomotion, zebrafish larvæ display successive turn and swim bouts
388 called episodes, interleaved with resting periods. This behavior can be analyzed by
389 semi-automated methods, making possible to distinguish between episodes based on
390 the average swim speed. Swimming episodes with a speed close to the overall average
391 speed of all recorded episodes are considered as cruises episodes or normal swim.
392 Episodes with a speed higher than twice the overall average speed of all recorded
393 swim episodes, are considered as fast episodes or bursts.

394 We first studied the dynamic of maturation of larval cruises and bursts episodes in
395 control conditions. We tracked the position of individual larvæ during 3 rounds of
396 10 minutes recordings at 4, 5, 6 and 7 dpf. The recorded parameters reflected a
397 gradual increase of spontaneous locomotion from 4 to 6 dpf and a relative stability
398 between 6 and 7dpf. From 4 to 6 dpf, the number of episodes, the duration of swimming
399 and distance covered increases, both for cruises and bursts episodes ($p<0.01$ for each
400 parameters, Bonferroni post-hoc test, $n=48$ individuals for each stages; Figure 4,
401 lighter blue boxplots). In contrast, between 6 and 7 dpf, the recorded parameters were
402 stable both for cruises and bursts episodes ($p=0.16$, 1 and 1 respectively; Figure 4,
403 darker blue boxplots). Based on these results, we concluded that we could set our
404 analysis window between 6 and 7 dpf.

405 **Effects of pharmacological treatments on the locomotion of 6-7 dpf larvæ.**

406 We next studied the effect of transient increase and decrease of ENE during the
407 embryonic period on locomotion recorded in larval zebrafish (Figure 5A). We recorded
408 spontaneous locomotion of 6-7 dpf zebrafish larvæ over 3 consecutive 10 minutes
409 sessions in 3 conditions: control, increased ENE, and decreased ENE. A
410 representative example of traces obtained for 24 well plates for each conditions is
411 shown in Figure 5B. For cruises and bursts episodes, the four parameters measured
412 were the number of swim bouts, the total duration of swim, the total distance covered,
413 the average speed of swim (Figure 5 C-J).

414 For cruises episodes, in control conditions, the four measured parameters were
415 the number of swim bouts: 1267.2+/-292.3, total duration: 306.5+/-58.6 s, total distance
416 covered: 767.5+/-285.1 mm and average speed: 2.5+/-0.7 $mm.s^{-1}$ (n=318 larvæ from
417 15 independent experiments, Figure 5B-F, blue boxplots).

418 The number of swim bouts was decreased following both the increase and the
419 decrease of ENE (-5.8+/-2.3% ; -22+/-5% respectively, Figure 5C). The three other
420 parameters increased either after an increase or a decrease of ENE (the total duration:
421 +4.6+/-2.1% ; +35.4+/-5.8%; the total distance covered: +38.3+/-4.9% ; +14.7+/-4.3%
422 and average speed: +34,6+/-4.8% ; +22.2+/-5% respectively, $p<0.01$ conover posthoc
423 comparisons; n>262 larvæ from 15 independent experiments; Figure 5D-F).

424 For bursts episodes, in control conditions, the 4 parameters studied were the
425 number of swim bouts: 301+/-227.6, the total duration: 42+/-38.4 s, the total distance
426 covered: 434.2+/-492.6 mm and the average speed of swim: 9.7+/-2.8 $mm.s^{-1}$
427 (Figure 5 G-J, blue boxplots).

428 Three of these parameters changed according to the treatments. They increased
429 following an increase of ENE and decreased following a decrease of ENE (number of
430 swim bouts: +24.6+/-4%;-54.8+/-6%; total duration: +37.8+/-4.8%;-58+/-6%; total
431 distance covered: +58.8+/-5%;-61.6+/-5.9% respectively, % of change followed by the
432 confidence interval, n>262 larvæ from 15 independent experiments; p<0.01 conover
433 posthoc comparisons, Figure 5G-J). Average speed also increased following a
434 increase of ENE (+17+/-3.8% Figure 5J, green boxplot) while it did not change
435 following a decrease of ENE (Figure 5J, red boxplot).

436 These results showed that the consequences of perturbing the embryonic
437 electrical excitability are different on the cruises episodes and on bursts episodes,
438 suggesting that the underlying neural networks of these swimming modes are not the
439 same and/or that they are not regulated in the same way following changes in ENE.

440 **Kinetics of the direct effects of acute pharmacological treatments on the**
441 **locomotion of 6-7 dpf larvæ.**

442 To exclude a direct effect of the drugs used on the larvæ locomotion, we next
443 followed the time course of the effects of acute pharmacological treatments (veratridine
444 and TCNF) in 6-7 dpf larvæ. We performed 10 minutes recording sessions before
445 application of the treatments, then +2 hours, and 24 hours after the treatments.

446 For cruises episodes, the results obtained following acute veratridine applications
447 are close from the one induced by the embryonic applications with a decrease of the
448 number of episodes and an increase of the duration and the distance. Only the results
449 for the average speed are different since it was not significantly different following acute
450 application while it increased following embryonic application (Figure 6A-D green
451 boxplots). Following T.C.N.F applications the number of events decreased like similarly

452 as following embryonic application while duration, distance and average speed
453 remained unchanged (Figure 6A-D red boxplots).

454 For bursts episodes, acute treatments had overall similar effects on the recorded
455 parameters as the one recorded after treatments performed in 2-3 dpf embryos (Figure
456 6). Veratridine application induced an increase of duration and distance, while the
457 number of events and the average speed were not significantly different (Figure 6E-H
458 green boxplots). T.C.N.F application led to a decrease of number of events, duration
459 and distance during bursts, only the average speed remained unchanged
460 (Figure 6E- H red boxplots).

461 By the next day, while some of the effects of the acute treatments are still
462 detectable, all the effects of these treatments on bursts episodes had faded away
463 (Figure 6E-H, lighter colored boxplots). These results clearly show that the delay
464 between the embryonic treatments and our analysis of larval locomotion is longer than
465 the time required for the disappearance of the acute effect of the drugs. Hence, these
466 results support the existence of a long-term effect related to changes in electrical
467 activity during the embryonic period in the zebrafish.

468 ## Discussion (1261 / 1500w)

469 *Summary*

470 Immature forms of excitability, referred to here as Embryonic Neuronal Excitability
471 (ENE), including calcium spikes and activation of non-synaptic receptors to
472 neurotransmitters, contribute to modulate neuronal differentiation. Here we show that
473 the developing zebrafish is a suitable model to manipulate ENE using pharmacological
474 treatments and to study the consequences of these manipulations on the plasticity of
475 neuromodulator systems, at works in the pathogenesis of several human
476 neuropsychiatric diseases. Indeed, we report that ENE exerts a positive regulatory
477 effect on the specification of the dopaminergic phenotype by increasing the number of
478 dopamine cells in the telencephalon. The pharmacological manipulation of ENE has
479 also a clear behavioral outcome by changing the occurrence of high-speed episodes
480 of swimming in zebrafish larvæ.

481 *Balneation treatments and ENE*

482 For the present study, zebrafish embryos were exposed to pharmacological
483 compounds by means of balneation treatments. This methodological approach allows
484 performing global and transient drugs applications, relevant to natural situations where
485 embryos can be exposed to various biologically active or toxic compounds. Zebrafish
486 is highly suitable for such questions because of its external development in an egg,
487 and because its blood brain barrier is not fully mature until 10 dpf, allowing diffusion of
488 the drugs to the neuronal tissues. As a consequence, we were able to analyze
489 alterations by pharmacological treatments of calcium transients, one of the main form
490 of immature excitability.

491 We focused on calcium transients to assess the effectiveness of the treatments, but
492 other intercellular communication processes such as the paracrine activation of GABA

493 and glutamate receptors by endogenous transmitters are also likely perturbed by the
494 treatments. Further studies are required to decipher the specific contribution of each
495 of these mechanisms to the cellular and behavioral effects we reported here.

496 *Calcium transients in the zebrafish forebrain*

497 One reason to focus on calcium transients is that they have been involved in
498 neurotransmitter phenotype specification in other models of neuronal plasticity. In
499 addition, calcium transients are conveniently measured by calcium imaging.

500 Calcium transients were already reported in the spinal cord of zebrafish embryos
501 around 24 hpf. Here, recordings were performed in the forebrain of embryonic
502 zebrafish around 48 hpf, a time at which the transition toward synaptic network activity
503 has occurred in the spinal cord. These observations are in accordance with the
504 existence of an postero-anterior gradient of neuronal maturation, similar to what was
505 described in xenopus.

506 Calcium transients in the forebrain had frequency and duration similar to what has
507 been described in the zebrafish spinal cord. This duration is overall shorter than what
508 has been observed in the Xenopus nervous system. The basis of these interspecies
509 differences are not known, but it suggests that the duration of the transients is not
510 necessarily the pertinent signal to trigger the effect on neuronal differentiation. This is
511 further suggested by the results of the TCNF treatments reported here, which lead to
512 changes in DA specification and in locomotion parameters, while the duration of
513 individual spikes duration was not changed.

514 We chose to drive the expression of GCamp by an exogenous trigger, here a heat-
515 shock. This allowed the expression of the calcium reporter in all the cells present at
516 the selected period of recordings. The next step of our approach will thus be to use
517 differentiation markers of the DA lineage to identify the differentiation status of the cells

518 where the Ca^{2+} spikes are detected, and also to see whether there are different
519 dynamics of the calcium transients between different subregions of interest in the
520 embryonic brain by using whole brain calcium imaging.

521 *Identification of a biomarker for DA reserve pool neurons?*

522 The effect of ENE perturbations on the DA phenotype analyzed by the number of
523 TH1+ cells was in agreement with the homeostatic rule described in xenopus. Indeed,
524 DA phenotype was enhanced by increased excitability, as expected from an overall
525 inhibitory neurotransmitter. The relative constancy of the number of vMAT2+ cells,
526 together with the absence of significant change is caspase 3-labelled cells upon
527 treatments, suggest that modulation of excitability did not affect cell death or
528 proliferation, but rather triggered a plasticity of the dopaminergic phenotype. This
529 plasticity of the DA phenotype is likely to occur within the pool of vMAT2+ cells, since
530 the number of VMAT2+/TH+ was increased with increased excitability, at the expense
531 of VMAT2+/TH- cells. Therefore, the VMAT2+/TH- cells would be a reserve pool of
532 cells primed to become dopamine neurons when plasticity-triggering events occur.
533 Although somewhat peculiar at first sight, the expression of the vesicular transporter
534 in a reserve pools of cells, might have a functional advantage in term of response to
535 plasticity-triggering events, limiting the number of factors to be changed for reaching a
536 fully functional dopamine phenotype.

537 *Behavioral consequences of ENE*

538 Perturbations of ENE had also behavioral consequences in zebrafish larvæ. For
539 bursts episodes, the initiation of movement is likely to be the prime parameter modified
540 following ENE perturbations. Interestingly, hyperlocomotion is an endophenotype
541 related to ADHD and schizophrenia in zebrafish (Blin et al., 2008; Lange et al., 2018).
542 Determining whether a direct activation of TelDA cells could trigger an increase of

543 bursts episodes is an interesting perspective for the future, as seeing whether other
544 behaviors related to ADHD and schizophrenia such as prepulse inhibition are also
545 affected by alterations of ENE.

546 *Critical period for the effect of ENE perturbations*

547 We observed an effect of the pharmacological treatments performed during the
548 embryonic period on spontaneous locomotion several days after the end of the
549 treatments. In contrast, no effects were observed 24 hours after treatments performed
550 at 6 dpf in the zebrafish larvæ. These long-lasting effects of treatments at specific
551 embryonic time are in line with the existence of a critical developmental period, more
552 sensitive to homeostatic perturbations, promoting therefore significant phenotypic
553 plasticity in immature neurons. Interestingly, dopaminergic systems have multiple
554 functional role and are particularly prone to plasticity events, suggesting that these
555 systems might be a key factor for adaptability of the animals to environmental changes.
556 Whether it is a cause, a consequence or a simple correlation of their conservation
557 throughout animal evolution is still an open question.

558 *Potential involvement of changes of ENE in the pathogenesis of brain disease*

559 According to the 'Developmental Origins of Health and Disease (DOHaD)
560 hypothesis, transient exposure to perturbations during the development could lead to
561 emergence of disease in young or adult individuals (Mandy & Nyirenda, 2018).
562 Neurological and psychiatric diseases, such as autism spectrum disorders, ADHD, or
563 schizophrenia are hypothesized to have a developmental origin. The environmental
564 factors potentially contributing to these pathologies include malnutrition, stress, and
565 drugs exposure during the embryonic period.

566 Results from epidemiological studies and experiments in rodents further suggest
567 that a range of functional and behavioral abnormalities observed in the mature system

568 result from early alterations of dopaminergic neurons differentiation. The data
569 presented here point to an implication of ENE in the regulation of dopaminergic
570 differentiation in the developing brain, suggesting that ENE could act as an
571 intermediate between environmental factors and the molecular changes leading to the
572 alteration of dopamine-related behaviors.

573 These results provide a firm basis to dissect further the cellular and molecular
574 mechanisms linking exposure to external challenges with the subsequent changes in
575 ENE, in the maturation of the dopaminergic systems and its behavioral outputs. A
576 comparative study of the transcription factors differentially expressed in vMAT2 cells
577 following changes in ENE, would help identify dopaminergic related factors having an
578 activity-dependent expression, including epigenetic effectors (level of methylation,
579 histone acetylation).

580 Such mechanisms are underlying phenotypes related to ADHD and schizophrenia
581 in zebrafish, and opens new avenues to better understand how environmental factors
582 could promote developmental brain disorders such as schizophrenia and ADHD.

583 Bibliography

584 Blankenship AG & Feller MB (2010) Mechanisms underlying spontaneous patterned
585 activity in developing neural circuits. Nat.Rev.Neurosci. 11:18–29.

586 Blin M, Norton W, Bally-Cuif L, Vernier P, Laure B-C & Vernier P (2008) NR4A2
587 controls the differentiation of selective dopaminergic nuclei in the zebrafish brain.
588 Molecular and cellular neurosciences 39:592–604.

589 Borodinsky LN, Root CM, Cronin JA, Sann SB, Gu X & Spitzer NC (2004) Activity-
590 dependent homeostatic specification of transmitter expression in embryonic
591 neurons. Nature 429:523–530.

592 Crepel V, Aronov D, Jorquera I, Represa A, Ben-Ari Y & Cossart R (2007) A
593 parturition-associated nonsynaptic coherent activity pattern in the developing
594 hippocampus. Neuron 54:105–120.

595 Demarque M, Represa A, Becq H, Khalilov I, Ben-Ari Y & Aniksztejn L (2002)
596 Paracrine intercellular communication by a Ca2+- and SNARE-independent
597 release of GABA and glutamate prior to synapse formation. Neuron 36:1051–
598 1061.

599 Demarque M & Spitzer NC (2010) Activity-Dependent Expression of Lmx1b
600 Regulates Specification of Serotonergic Neurons Modulating Swimming
601 Behavior. Neuron 67:321–334.

602 Dulcis D, Jamshidi P, Leutgeb S & Spitzer NC (2013) Neurotransmitter switching in
603 the adult brain regulates behavior. Science 340:449–453.

604 Dulcis D, Lippi G, Stark CJ, Do LH, Berg DK & Spitzer NC (2017) Neurotransmitter
605 Switching Regulated by miRNAs Controls Changes in Social Preference. Neuron
606 95:1319-1333.e5.

607 Dulcis D & Spitzer NC (2008) Illumination controls differentiation of dopamine
608 neurons regulating behaviour. Nature 456:195–201.

609 Dulcis D & Spitzer NC (2012) Reserve pool neuron transmitter respecification: Novel
610 neuroplasticity. Developmental Neurobiology 72:465–474.

611 Gawel K, Banono NS, Michalak A & Esguerra C V. (2019) A critical review of
612 zebrafish schizophrenia models: Time for validation? Neuroscience and
613 Biobehavioral Reviews 107:6–22.

614 Gomez TM, Robles E, Poo M & Spitzer NC (2001) Filopodial calcium transients

615 promote substrate-dependent growth cone turning. Science 291:1983–1987.

616 Gomez TM & Spitzer NC (1999) In vivo regulation of axon extension and pathfinding
617 by growth-cone calcium transients. Nature 397:350–355.

618 Klein MO, Battagello DS, Cardoso AR, Hauser DN, Bittencourt JC & Correa RG
619 (2019) Dopamine: Functions, Signaling, and Association with Neurological
620 Diseases. Cellular and Molecular Neurobiology 39:31–59.

621 Lange M, Froc C, Grunwald H, Norton WHJ & Bally-Cuif L (2018) Pharmacological
622 analysis of zebrafish lphn3.1 morphant larvae suggests that saturated
623 dopaminergic signaling could underlie the ADHD-like locomotor hyperactivity.
624 Progress in Neuro-Psychopharmacology and Biological Psychiatry 84:181–189.

625 Lange M, Norton W, Coolen M, Chaminade M, Merker S, Proft F, Schmitt A, Vernier
626 P, Lesch K-P & Bally-Cuif L (2012) The ADHD-linked gene Lphn3.1 controls
627 locomotor activity and impulsivity in zebrafish. Molecular psychiatry 17:855.

628 Ma PM (1994a) Catecholaminergic systems in the zebrafish. I. Number, morphology,
629 and histochemical characteristics of neurons in the locus coeruleus. Journal of
630 Comparative Neurology 344:242–255.

631 Ma PM (1994b) Catecholaminergic systems in the zebrafish. II. Projection pathways
632 and pattern of termination of the locus coeruleus. Journal of Comparative
633 Neurology 344:256–269.

634 Ma PM (1997) Catecholaminergic systems in the zebrafish. III. Organization and
635 projection pattern of medullary dopaminergic and noradrenergic neurons.
636 Journal of Comparative Neurology 381:411–427.

637 Ma PM (2003) Catecholaminergic systems in the zebrafish. IV. Organization and

638 projection pattern of dopaminergic neurons in the diencephalon. Journal of
639 Comparative Neurology 460:13–37.

640 Mandy M & Nyirenda M (2018) Developmental Origins of Health and Disease: the
641 relevance to developing nations. International health 10:66–70.

642 Murray RM, Bhavsar V, Tripoli G & Howes O (2017) 30 Years on: How the
643 Neurodevelopmental Hypothesis of Schizophrenia Morphed Into the
644 Developmental Risk Factor Model of Psychosis. Schizophrenia Bulletin 43:1190–
645 1196.

646 Owens DF & Kriegstein AR (1998) Patterns of intracellular calcium fluctuation in
647 precursor cells of the neocortical ventricular zone. Journal of Neuroscience
648 18:5374–5388.

649 Owens DF & Kriegstein AR (2002) Is there more to GABA than synaptic inhibition?
650 Nat.Rev.Neurosci. 3:715–727.

651 Plazas P V, Nicol N & Spitzer NC (2013) Activity-dependent competition regulates
652 motor neuron axon pathfinding via PlexinA3. Proceedings of the National
653 Academy of Sciences of the United States of America 110:1524–1529.

654 Scain AL, Le Corronc H, Allain AE, Muller E, Rigo JM, Meyrand P, Branchereau P &
655 Legendre P (2010) Glycine release from radial cells modulates the spontaneous
656 activity and its propagation during early spinal cord development. Journal of
657 Neuroscience 30:390–403.

658 Schweitzer J & Driever W (2009) Development of the dopamine systems in zebrafish.
659 Adv Exp Med Biol 651:1–14.

660 Schweitzer J, Löhr H, Filippi A & Driever W (2012) Dopaminergic and noradrenergic

661 circuit development in zebrafish. Developmental Neurobiology 72:256–268.

662 Spitzer NC, Kingston PA, Manning TJ & Conklin MW (2002) Outside and in:
663 development of neuronal excitability. Curr.Opin.Neurobiol. 12:315–323.

664 Tay TL, Ronneberger O, Ryu S, Nitschke R & Driever W (2011) Comprehensive
665 catecholaminergic projectome analysis reveals single-neuron integration of
666 zebrafish ascending and descending dopaminergic systems. Nature
667 Communications 2:112–171.

668 Warp E, Agarwal G, Wyart C, Friedmann D, Oldfield CS, Conner A, Del Bene F,
669 Arrenberg AB, Baier H, Isacoff EY, Bene F, Arrenberg AB, Baier H & Isacoff EY
670 (2012) Emergence of patterned activity in the developing zebrafish spinal cord.
671 Current Biology 22:93–102.

672 Yamamoto K, Ruuskanen JO, Wullimann MF & Vernier P (2011) Differential
673 expression of dopaminergic cell markers in the adult zebrafish forebrain. The
674 Journal of comparative neurology 519:576–598.

675

Figure legends

Figure 1 Presence of calcium spikes in the zebrafish telencephalon and their manipulations by transient balneation in pharmacological agents.

A. Consecutive images of a confocal time series of the brain of 48 hpf of Et(hsp:gal4;UAS:GCamp6f) embryos in control conditions. Fluorescence is displayed on a pseudocolor scale, the look up images intensity scale coding is shown in the right corner of the first image. Scale bar is 100µm. White dash circle surround the cell body of a cell displaying a calcium transient.

B. Changes in fluorescence intensity are plotted as a function of time. Ca2+ transients were scored for fluorescence changes, more than two times the SD of the baseline (dashed lines), and >3 sec in duration, calculated as the width at half-maximum. Representative traces from control conditions (in blue), following veratridine treatment (in green) and following treatment with a pharmacological cocktail containing TTX (2.5 µM), ω-Conotoxin (0.1 µM), Nifedipine (0.5 µM) and Flunarizine (2.5 µM) (TCNF, in red).

C. Left, boxplots showing the mean duration of single calcium spikes in control conditions (in blue, 3.3+/-1.6 sec), following veratridine treatment (in green, 3.7+/-1.7 sec) and following TCNF treatment (in red, 3.4+/-1.4 sec).

Middle, boxplots showing the mean frequency of calcium transients in control conditions (in blue, 6.6+/-5.4 spikes per hour, n=28 cells from 5 independent preparations), following veratridine treatment (in green, 9.2+/-6.6 spikes per hour, n=36 cells form 4 independent preparations) and following TCNF treatment (in red, 4.7+/-3 spikes per hour, n=17 cells form 4 independent preparations).

Right, boxplots showing the mean incidence of single calcium spikes in control conditions (in blue, 45.2+/-9.7%, n=5 independent preparations), following veratridine treatment (in green, 58.8+/-9.7%, n=4 independent preparations) and in the presence of TCNF (in red, 4.7+/-3 spikes per hour, n=17 cells form 4 independent preparations).

Figure 2 Effects of 24hrs balneation treatment on the number of dopaminergic neurons in the zebrafish larval telencephalon and OB.

A. Maximum projection of confocal z series of the brain of 6-7 dpf Et(VMAT2:eGFP) larvæ, in control conditions (left column boxed in blue), in the presence of veratridine (middle column, boxed in green) and in the presence of TCNF (right column, boxed in red). Immunostaining to TH (magenta) and GFP (cyan) and DAPI (yellow) are shown as merge and individual channels. Scale bars = 50 µm.

B-E. Boxplots showing the mean number of IR cells in control conditions, in the presence of veratridine and in the presence of “TCNF” in the telencephalon (B,C) and in the olfactory bulb (C,D), for TH (B,D) and for GFP (vMAT2 cells, C,E).

Figure 3 Absence of changes in cell death following increase or decrease of ENE

A. Maximum projection of confocal z series of the brain of 6-7 dpf Et(VMAT2:eGFP) larvæ, in control conditions (left image boxed in blue), in the presence of veratridine (middle image, boxed in green) and in the presence of TCNF (right image, boxed in red). Immunostaining to caspase-3 (magenta) and GFP (cyan) are shown as merged channels. Scale bars = 50 µm.

B. Boxplots showing the mean number of IR cells in control conditions, in the presence of veratridine and in the presence of “TCNF” for the caspase-3 staining in the olfactory bulb and the telencephalon.

Figure 4 Maturation of locomotion parameters

A-H. Boxplots showing the mean of 4 swimming parameters, number of episode (A,E), total duration (B,F), distance covered during swimming (C,G) and speed (D,H) for cruises episodes (A-D) and for bursts episodes (E-H) at different stage of larval development (4, 5, 6, and 7dpf).

Figure 5 Effects of 24hrs balneation treatments during embryonic development on spontaneous swimming of zebrafish larvæ.

A. Time line of the experiments indicating the timing (in days post fertilization, dpf) for the pharmacological treatments, and the following locomotion tests.

B. Representative path reconstructions for 24 individual larvæ during a 10 minutes trial for three experimental conditions. The portion of the path corresponding to bursts episodes (shown in red) are longer when early activity is increased (veratridine treatment) and shorter when early activity is decreased (T.C.N.F. treatment).

C-J. Boxplots showing the mean of different swimming parameters in different experimental conditions, Mean number of episode (C,G), total duration (D,H), distance covered during swimming (E,I) and speed (F,J) are shown for cruises episodes (C-F) and for bursts episodes (G-J).

Figure 6 Effects of 2hrs acute balneation treatments on zebrafish spontaneous swimming.

A-H. Boxplots showing the mean of different swimming parameters, mean number of episode (A,E), total duration (B,F), distance covered during swimming (C,G) and speed (D,H), for cruises episodes (A-D) and for bursts episodes (E-H), in different experimental conditions. The effects of 2hrs acute treatments with DMSO,

Veratridine, or TCNF are compared to pre-application recordings and 24hrs post-application recordings.

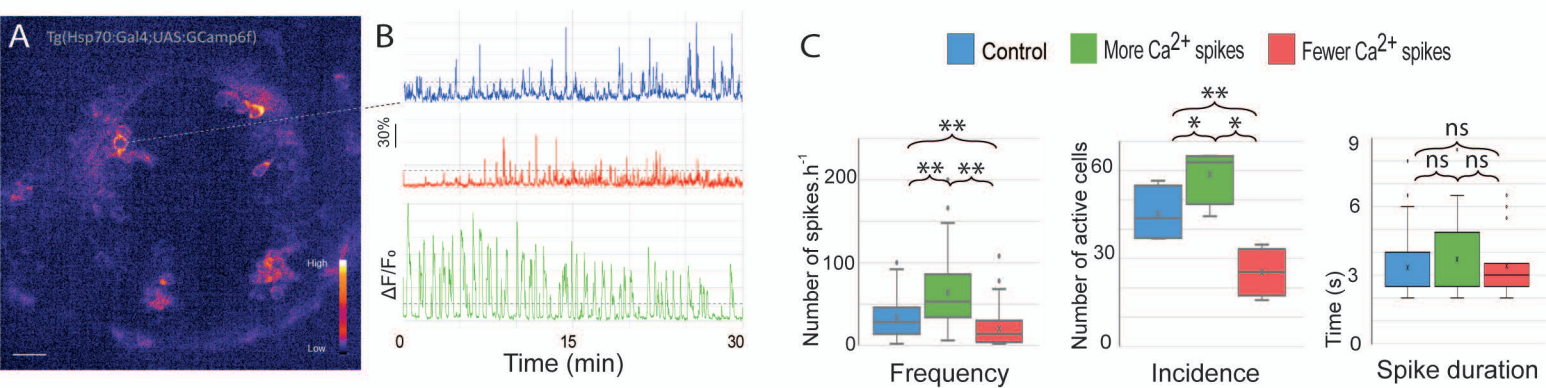

Bataille et al., Figure 1. Calcium spikes and their modulation by pharmacological treatments, in the embryonic zebrafish forebrain

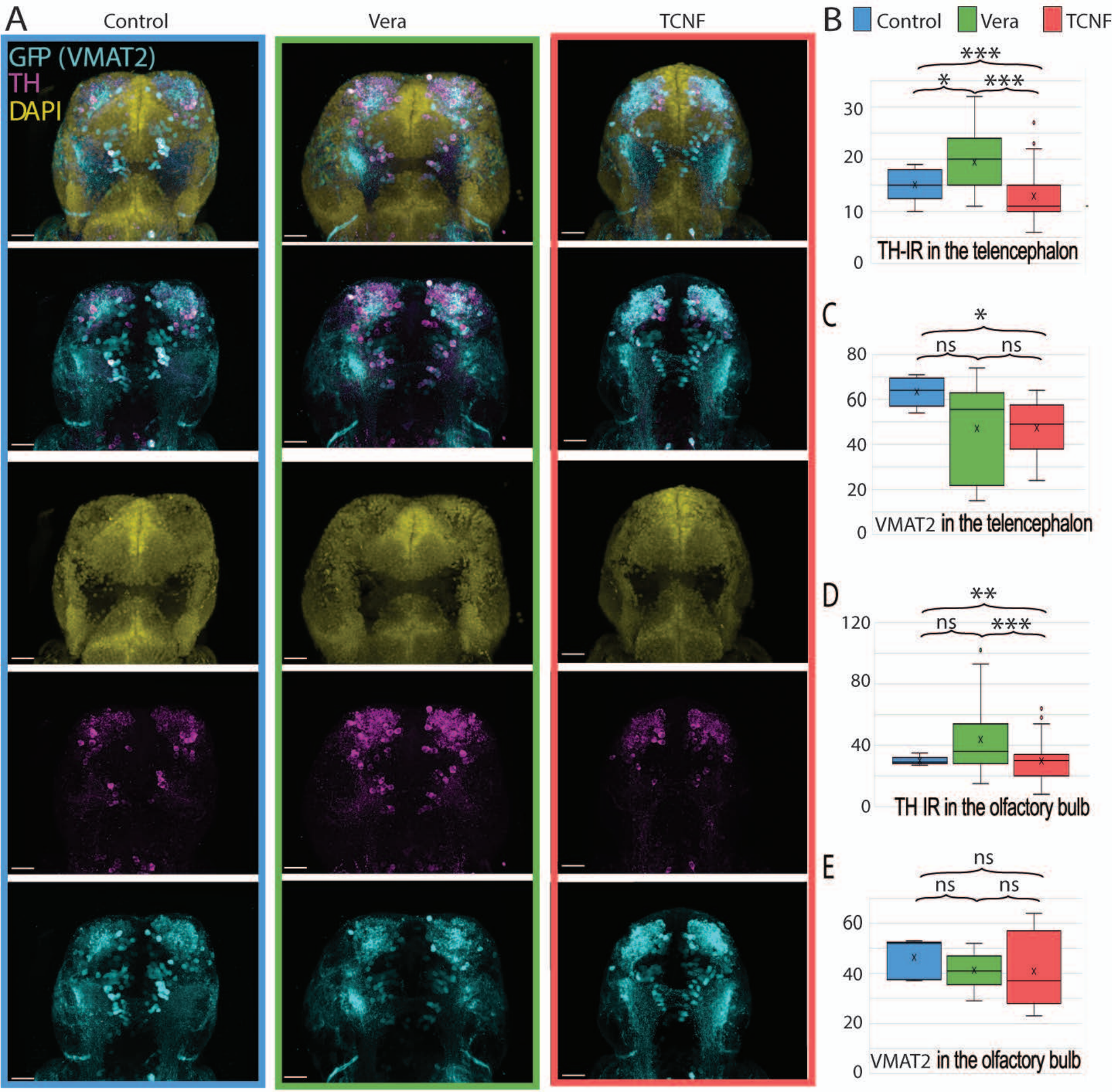

Bataille et al., Figure 2. Effects of ENE on the numbre of DA neurons in the zebrafish forebrain

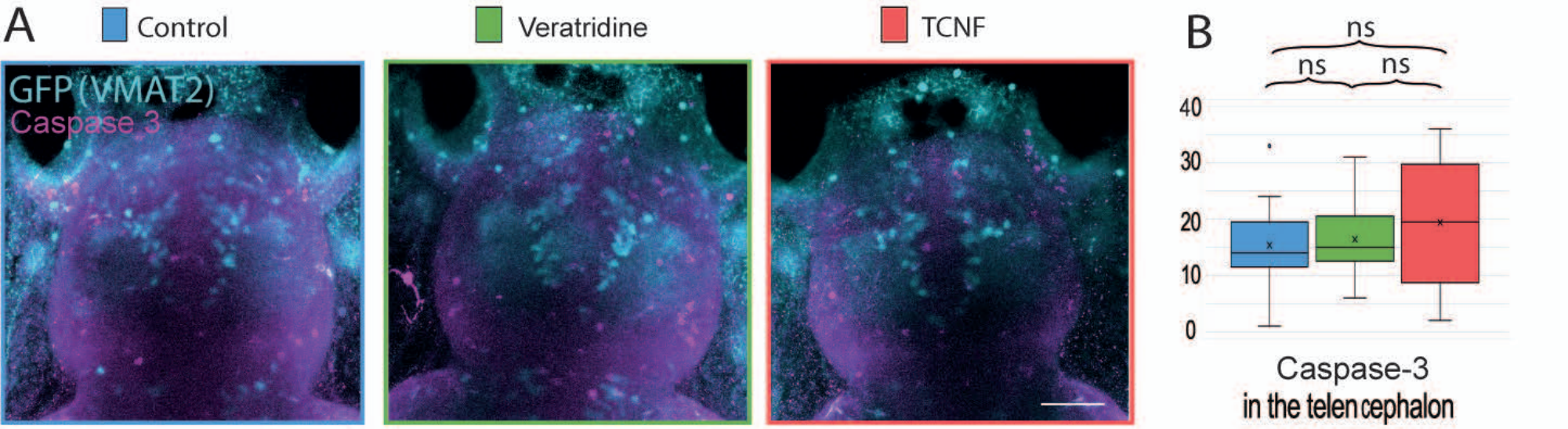

Bataille et al., Figure 3. Effects of ENE on caspase-3 expression in the larval zebrafish forebrain

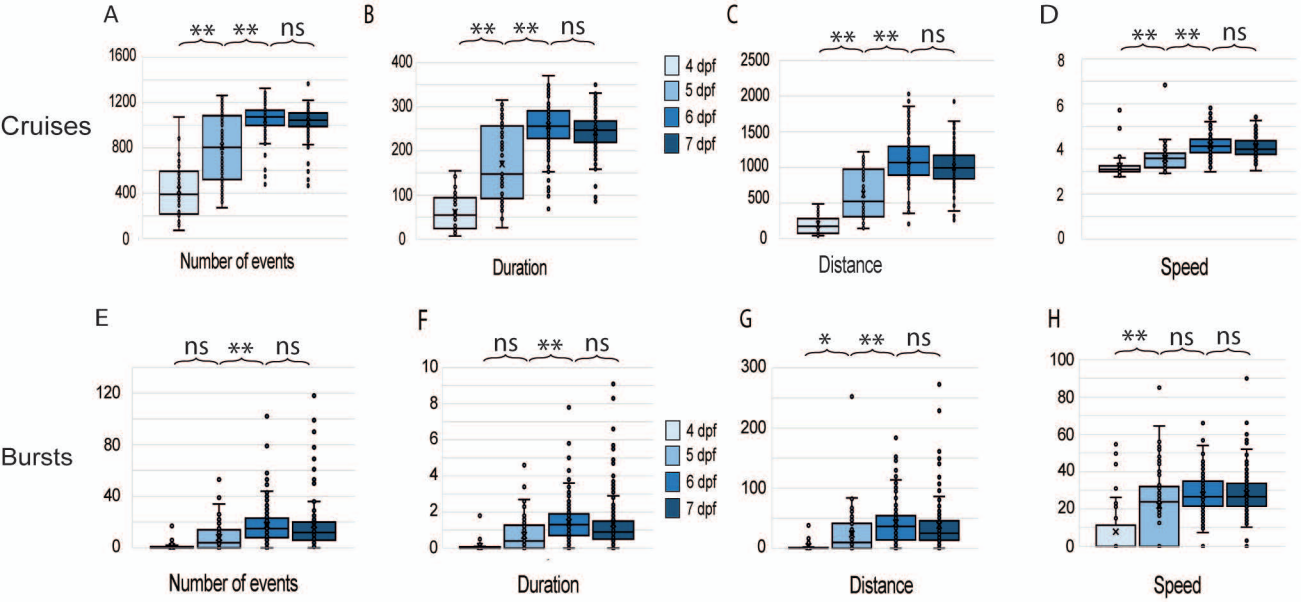

Bataille et al., Figure 4. Development of zebrafish spontaneous locomotion

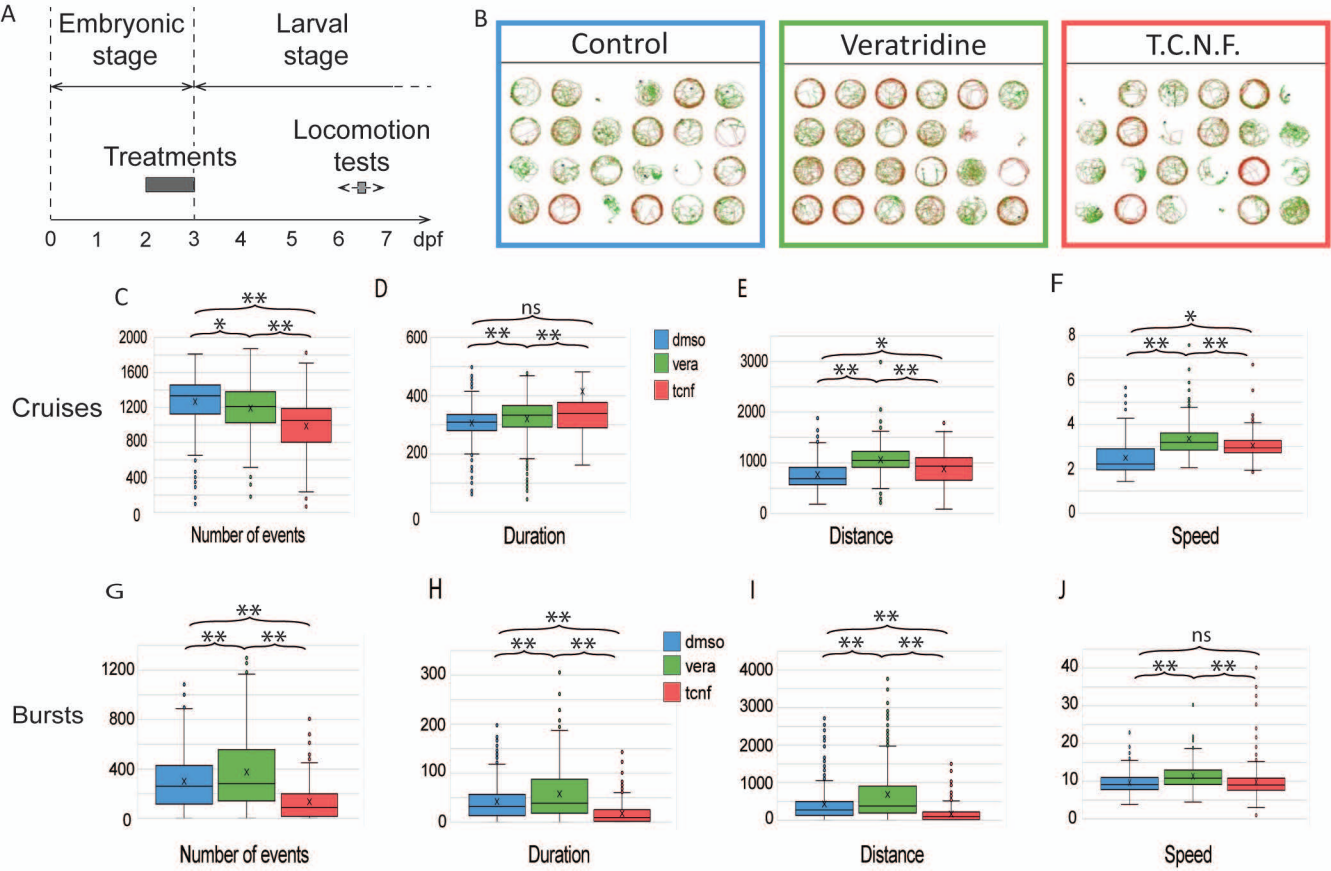

Bataille et al., Figure 5. Effects of ENE on the zebrafish spontaneous locomotion

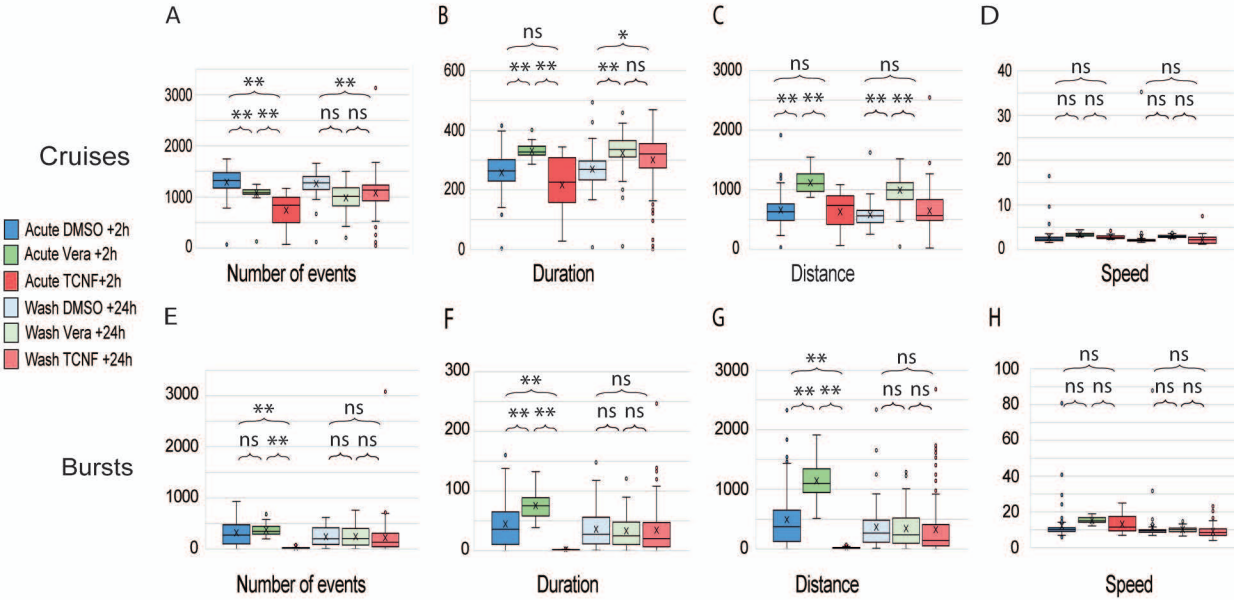

Bataille et al., Figure 6. Effects of acute pharmacological treatments on the zebrafish spontaneous locomotion